Pediatr Radiol (2009) 39:1–16
DOI 10.1007/s00247-008-0917-7

REVIEW

Imaging of congenital diaphragmatic hernias

George A. Taylor · Omolola M. Atalabi · Judy A. Estroff

Received: 20 March 2008 / Revised: 28 April 2008 / Accepted: 19 May 2008 / Published online: 8 July 2008

Abstract Congenital diaphragmatic hernias are complex and life-threatening lesions that are not just anatomic defects of the diaphragm, but represent a complex set of physiologic derangements of the lung, the pulmonary vasculature, and related structures. Imaging plays an increasingly important role in the care of these infants. Prenatal sonography and MRI have allowed early and accurate identification of the defect and associated anomalies. These tools have also been the key to defining the degree of pulmonary hypoplasia and to predicting neonatal survival and need for aggressive respiratory rescue strategies. In the postnatal period, conventional radiography supplemented by cross-sectional imaging in selected cases can be very useful in sorting out the differential diagnosis of intrathoracic masses, in the detection of associated anomalies, and in the management of complications. Understanding the pathogenesis of diaphragmatic defects, the underlying physiologic disturbances, and the strengths and limitations of current imaging protocols is essential to the effective and accurate management of these complex patients.

Keywords Congenital diaphragmatic hernia · Prenatal · Imaging

G. A. Taylor (✉) · O. M. Atalabi · J. A. Estroff
Department of Radiology, Children's Hospital Boston,
Harvard Medical School,
300 Longwood Ave.,
Boston, MA 02115, USA
e-mail: george.taylor@childrens.harvard.edu

Present address:
O. M. Atalabi
The College of Medicine/University College Hospital,
Ibadan, Nigeria

Introduction

Congenital diaphragmatic hernias (CDH) are serious and life-threatening anatomic lesions that are frequently associated with additional anatomic malformations, syndromes, and chromosomal anomalies. Despite a number of recent advances in prenatal diagnosis, intrapartum treatment and postnatal management, diaphragmatic hernias remain an important cause of perinatal morbidity and mortality worldwide [1, 2]. Early prenatal diagnosis of the primary lesion and associated anomalies is important for appropriate obstetric and postnatal surgical planning. Thus, familiarity with the pathogenesis and prenatal and postnatal imaging appearance of the various types of diaphragmatic hernia is important for the multidisciplinary medical and surgical team taking care of these patients. In this essay, we review and update the imaging features of diaphragmatic defects with emphasis on early and accurate identification of high-risk and complex lesions.

Development

The human diaphragm begins to develop at about the fourth week of gestation with the formation of lateral pleuroperitoneal cavities that communicate cranially and laterally with the unpaired pericardial cavity and the extraembryonic celom, respectively. It is formed from components of the transverse septum, the mediastinum, pleuroperitoneal membrane, and the musculature of the lateral body wall. The pleuroperitoneal folds grow medially and ventrally until the seventh week of gestation when they fuse with the septum and the mediastinum. Muscularization of the primitive diaphragm then begins with the migration of myoblasts

from the cervical myotomes, leading to incorporation of the intercostal muscles with the diaphragm. A fibrous lumbocostal trigone remains as a remnant of the pleuroperitoneal membrane at the intersection of the lumbar and intercostal muscles in the posterolateral portion of each hemidiaphragm (Fig. 1) [3–5].

Pulmonary development is also very important in the understanding of CDH. The lungs begin their development as a ventral outpouching of the primitive foregut just after the third week of gestation, and they undergo successive branching until the sixteenth week. Thereafter, terminal bronchioles, acini and alveolar air sacs continue to develop throughout the remaining gestation and into childhood until approximately 8 years of age. Development of the pulmonary vasculature closely follows that of the airways and can also be affected by maldevelopment of the diaphragm.

Although knowledge of the embryologic causes of abnormalities of the diaphragm is useful in the understanding of the pathogenesis of diaphragmatic hernias, it does not form a clinically useful classification system. Hernias are more practically classified by their morphologic characteristics and location [3].

Bochdalek hernia

Pathogenesis

Posterolateral (foramen of Bochdalek) hernias occur with an estimated frequency of 1 per 2,000 to 5,000 live births [4]. Although most (80%) are left-sided, bilateral hernias have been reported but are rare. A true hernia sac might be present in up to 15% of hernias [4].

While the pathogenesis of CDH is not well understood, much more is known about the cellular events and molecular cues that control early differentiation of the diaphragm. Initial studies suggested that the primary abnormality resulting in CDH was a failure or delay of the pleuroperitoneal fold and transverse septum to properly fuse with the intercostal muscles by the eighth week of gestation [6]. More recent studies have suggested that diaphragmatic defects arise at an earlier stage with a malformation of the pleuroperitoneal fold [6]. A "mesenchymal hit" hypothesis has been proposed in an attempt to explain the association of CDH and other somatic defects. It states that similar signaling pathways are involved in the differentiation of mesenchymal cells in all affected structures, and that the function of these mesenchymal cells is disrupted by genetic or environmental triggers [7]. Transcription factors such as GATA-4 and its transcriptional coregulator FOG-2 have been implicated in normal mesenchymal cell function in the developing diaphragm and lungs in experimental models and in humans [8]. Defects in the mesenchymal substructure in these experimental animal models occur consistently in the posterolateral component of the fold and appear to have a strong causal relationship with subsequent maldevelopment of diaphragmatic musculature and CDH [9]. Exposure to environmental toxins such as the herbicide nitrofen (2,4-dichlorophenyl-*p*-nitrophenyl ether) results in malformations of the diaphragm that are very similar to those in infants with CDH. Vitamin A deficiency and inactivation of the Wilms tumor gene (wt1) also lead to equivalent defects. These studies suggest that a common pathway is an interference of the retinoid signaling pathway by inhibition of the enzyme retinaldehyde dehydrogenase [10].

Abnormalities in development of the diaphragm often affect the process of bronchial development, resulting in a reduced number of bronchial branchings and a diminished absolute number of alveoli, resulting clinically in pulmo-

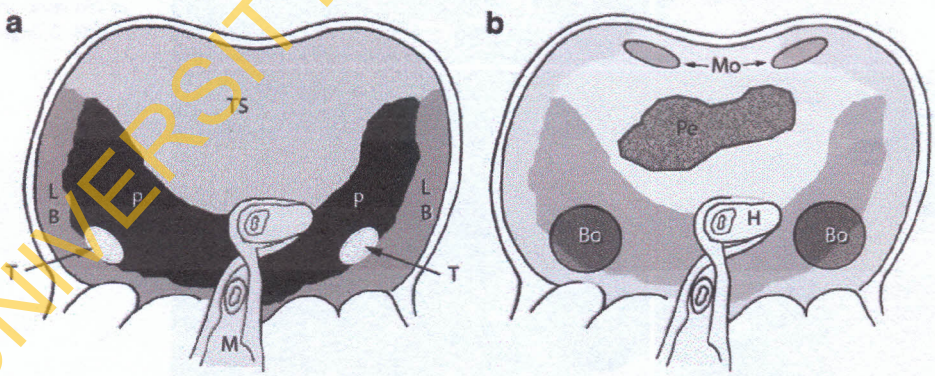

Fig. 1 Diagrams of developmental components of the fetal diaphragm. **a** Developmental components of the diaphragm include the transverse septum (*TS*), mediastinum (*M*), pleuroperitoneal membrane (*P*), lateral body wall musculature (*LB*), and the lumbocostal trigone (*T*). **b** Relationship of diaphragmatic hernias to developmental components of the diaphragm. Foramen of Bochdalek (*Bo*), foramen of Morgagni (*Mo*), pericardial defect (*Pe*), hiatal foramen (*H*) (diagrams modified from reference [3])

nary hypoplasia [2, 3]. Development of the pulmonary vasculature closely follows the airways and can be truncated in a similar fashion. Inappropriate extension and hyperplasia of muscle in small arterioles might also be present, contributing to postnatal pulmonary hypertension. These changes are often asymmetric, being more pronounced on the ipsilateral side.

Prenatal imaging evaluation

Sonography Sonography has been the mainstay of prenatal diagnosis of CDH for at least 20 years. Although CDH can be detected on routine sonography as early as 18 weeks, the mean gestational age at the time of detection is approximately 24 weeks [11] (Fig. 2). The sensitivity of sonography for prenatal detection of CDH varies from 18% to 87% in published series and appears to improve in the presence of associated, more readily observed anomalies, with advancing gestational age, and with increasing experience of the individual performing the examination [12]. In one multiinstitutional study in Europe, the detection rate for CDH increased from 51% in uncomplicated cases to 72% when CDH was associated with other malformations [11].

The typical sonographic features of a left CDH include the presence of a stomach bubble or left lobe of the liver at the level of the fetal heart, bowel loops in the fetal chest, and a right mediastinal shift. In addition, the abdomen is scaphoid, and the gallbladder and hepatic or umbilical veins might be in an abnormal position within the abdomen [12]. The echogenicity of the fetal lung and liver can be similar and difficult to distinguish on gray-scale sonography. Color Doppler sonography might be helpful in detailing the abnormal position and course of intrahepatic vessels. Bowing of the umbilical segment of the portal vein to the left of the midline and portal branches to the lateral segment of the left hepatic lobe coursing toward or above the diaphragmatic ridge are good predictors for liver herniation into the fetal thorax (positive predictive values of 85% and 100%, respectively) [13–15]. However, the fetal stomach is not always displaced into the chest, especially in fetuses with right-side CDH. These fetuses might have herniation of the gallbladder into the right chest, abnormal position of

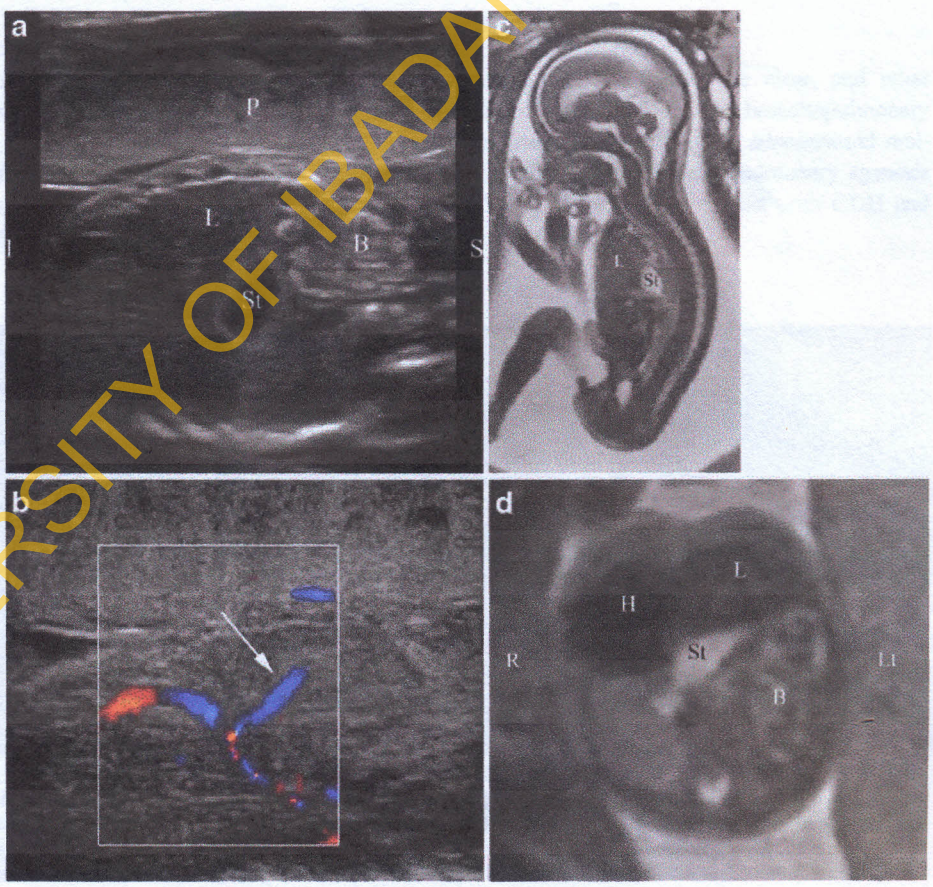

Fig. 2 Left Bochdalek hernia in a 20-week fetus. **a** Sagittal sonogram of the left fetal chest shows herniation of echogenic bowel (*B*), stomach (*St*) and liver (*L*) into the fetal chest (*P* placenta). **b** Color Doppler sonogram shows superior displacement of hepatic vessels (*arrow*) into the fetal chest. **c**, **d** Sagittal (**c**) and axial (**d**) FIESTA and T2-W MRI images of the fetus obtained on the same day show intrathoracic herniation of the liver (*L*), bowel (*B*) and stomach (*St*) with displacement of the heart (*H*) to the right side (*R* right, *Lt* left)

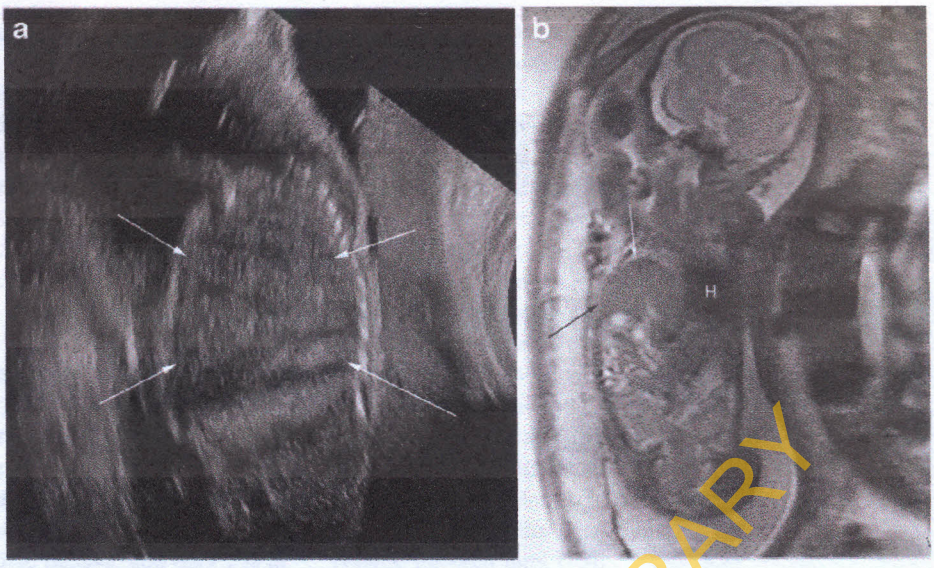

Fig. 3 Right Bochdalek hernia in a 20-week fetus. **a** Sagittal sonogram of the right fetal chest shows the liver filling the right hemithorax (*arrows*). **b** Coronal T2-W MR image obtained the same day confirms the presence of a right-side Bochdalek hernia with herniation of the liver and bowel (*arrows*) and displacement of the fetal heart (*H*) to the left

the intrahepatic portion of the umbilical vein, and mediastinal shift to the left [12].

MRI In fetuses suspected of having a CDH, MRI is often recommended to assess herniation of the liver and associated anomalies (Fig. 3). MRI has been shown to provide additional information to that obtained sonographically in 38% to 50% of fetuses with chest lesions [16, 17], and MRI affects clinical care in selected cases [16, 18–20].

One of the important contributions of prenatal MRI in this condition is the assessment of fetal lung volumes (FLV). Fast spin-echo T2-W sequences have been reported to have a high degree of reproducibility and interobserver agreement in estimating FLV in normal fetuses and in fetuses with CDH [21, 22].

Differential diagnosis

At times the diagnosis of CDH is not clear, and other diagnoses should be considered, such as bronchopulmonary foregut malformations, congenital cystic adenomatoid malformations, sequestrations, and primary pulmonary agenesis or hypoplasia. These lesions might coexist with CDH and influence surgical planning (Fig. 4).

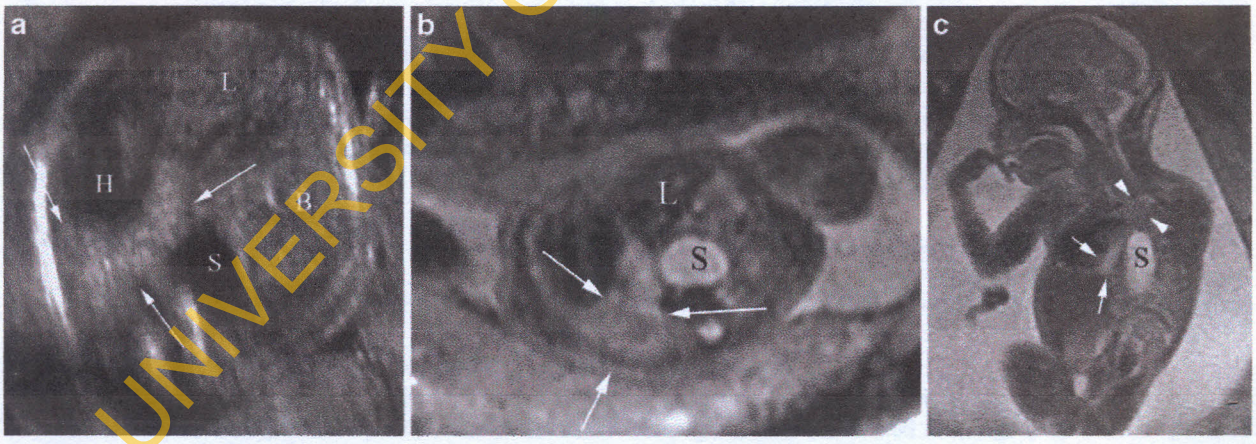

Fig. 4 Coexisting left Bochdalek hernia and sequestration in a 22-week fetus. **a** Axial sonogram of the fetal chest shows herniation of bowel (*B*), stomach (*S*), and liver (*L*) into the fetal chest, with displacement of the heart (*H*) to the right chest. An echogenic mass (*arrows*) is interposed between the heart and stomach. **a**, **b** Axial (**b**) and coronal (**c**) T2-W MR images of the fetus obtained on the same day confirm the presence of a thoracic mass (*arrows*) with signal intensity higher than that of compressed lung (*arrowheads*). A left lung sequestration was removed at postnatal repair of a CDH

Associated anomalies and complications

It is important to understand that the frequency of reported anomalies will vary markedly depending on the population studied. Associated anomalies are present in 25% to 50% of all patients with CDH and can be seen in up to 95% of stillborn infants with the disease [1, 23–26]. In addition to cleft palate, neural tube defects, and esophageal atresia, cardiac and genetic abnormalities are the most significant defects with respect to patient outcome [27, 28]. Cardiac malformations are present in 17% to 40% of fetuses with CDH and include hypoplastic left heart syndrome, tetralogy of Fallot, transposition of the great vessels, double-outlet right ventricle, and ventricular septal defects [1, 23–25]. Cardiac defects markedly increase neonatal mortality in children with CDH. In one study, the survival of CDH patients without heart disease was 70%, compared to 41% in children with associated cardiac defects, and only 5% in those with univentricular anatomy [26].

CDH is thought to be a sporadic malformation with little risk of recurrence. However, karyotyping is essential because 10–20% of these patients have chromosomal abnormalities. Trisomies 13, 18 and 21 and tetrasomy 12p (Pallister-Killian syndrome) are frequently associated genetic defects [23, 29]. Nearly 10% of children with CDH and associated anomalies have an underlying genetic syndrome such as the Fryns (CDH, coarse facies, micrognathia, macrostomia, and distal digital hypoplasia), Brachmann-De Lange (long eyelashes, confluent eyebrows, long philtrum, crescent-shape mouth) or a number of others [23].

A number of studies have assessed the value of prenatal sonographic findings to predict survival in patients with CDH. The likelihood of survival is lessened by the presence of an intrathoracic liver [30, 31], polyhydramnios [32], left-side hernia, size of low FLVs [33], and associated cardiac malformations [1].

Other prognostic features such as diagnosis made before 25 weeks of gestation, the presence of an intrathoracic stomach, and lung-to-head circumference ratio have not withstood the test of time as reliable prognostic indicators [34–36].

Determination of fetal lung volumes

Until recently, the lung-head ratio (LHR) was used as a measure of fetal lung hypoplasia and subsequent risk of respiratory failure. LHR is calculated using a two-dimensional measurement of the maximum area of the lung contralateral to the side of the hernia (obtained at the level of the atria on transverse images of the fetal lung, and expressed in square millimeters), divided by the head circumference (in millimeters). This ratio normalizes differences in lung volume related to gestational age. Although there continues to be a strong correlation between LHR and neonatal survival, this measure has not withstood the test of time as a reliable prognostic indicator, especially in fetuses without herniation of the liver into the chest [34–37]. Other studies have suggested that 3-D sonography or MR imaging is a better tool for determining the degree of pulmonary hypoplasia by direct measurements of total lung volume and for predicting neonatal mortality [14, 15].

MRI estimates of FLV are determined using a variation of the following technique:

T2-weighted half-Fourier single-shot fast spin-echo images are obtained using adjacent 4- to 5-mm-thick sections with no intersection gap. Images in the transverse plane of the lungs are used for planimetric measurements. Areas for each lung are determined by drawing free-hand regions of interest for each slice. Measured areas are added and multiplied by the slice thickness to determine the total volume for each lung [15].

The ratio of measured to expected FLV measured with 3-D US or MR imaging appears to be predictive of neonatal mortality in fetuses with CDH. FLVs in fetuses with CDH have been reported to be lower than age-matched control fetuses (median 0.34, range 0.16–0.66) [37]. In addition, fetuses with FLV measurements less than 15% to 25% of expected have a significantly higher mortality rate (19% vs. 40%), and fetuses in whom one lung could not be seen on MR imaging have a markedly lower likelihood of survival compared to those in whom both lungs are visible (18% vs. 62%) [18, 38].

Initial attempts to repair the defect antenatally were quickly abandoned because of the high risk of premature labor. In the early 1990s, experimental work by Wilson et al. [39] and DiFiore et al. [40] showed that tracheal ligation prevented pulmonary hypoplasia in fetal sheep with CDH [39, 40]. Subsequent randomized trials of laparoscopic tracheal ligation in humans in the United States were not able to show an improvement in survival. However, improvements in the technique by European practitioners have led to very encouraging results [41].

Postnatal imaging

Initial chest radiographs often show an opacified hemithorax with mass effect and contralateral shift of the mediastinum. Once air is introduced into the gastrointestinal tract, bowel gas is lacking in the abdomen and can be identified in the chest.

The location and course of vascular catheters and the nasogastric tube is altered in a high proportion of patients with CDH. The esophageal portion of the nasogastric tube deviates to the right in left-side CDH and to the left in right-side hernias. An intrathoracic nasogastric tube strongly suggests displacement of the stomach into the hernia. The

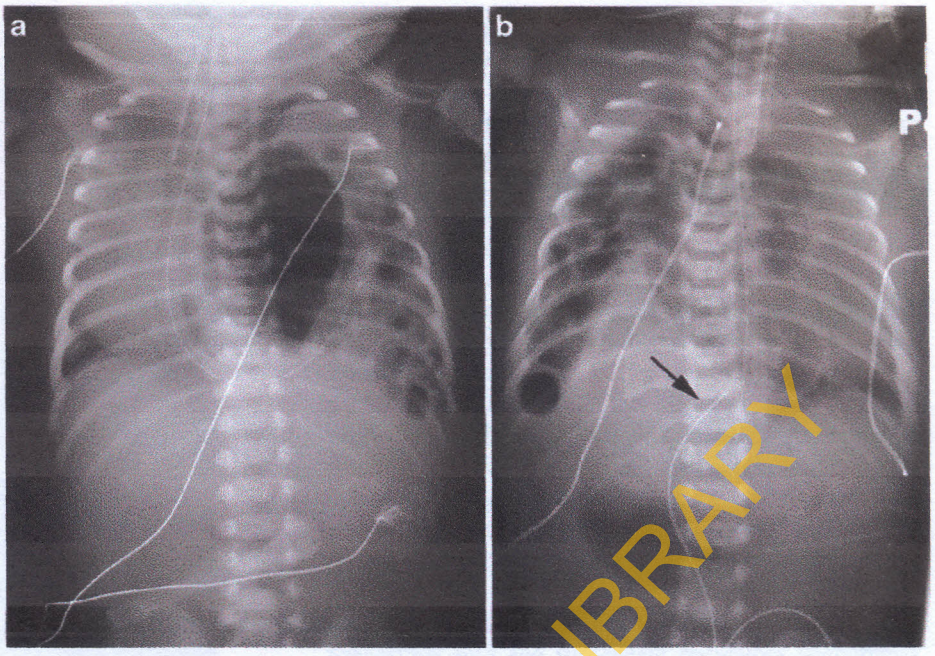

Fig. 5 Neonatal Bochdalek hernia. **a** A 1-day-old boy with left Bochdalek hernia. Chest radiograph shows deviation of the endotracheal tube and esophageal portion of the nasogastric tube to the right. Intrathoracic displacement of the nasogastric tube tip, bowel and stomach confirm the diagnosis of diaphragmatic hernia. **b** A 2-day-old girl with right Bochdalek hernia. Chest radiograph shows deviation of the nasogastric tube and umbilical venous catheter (*arrow*) to the left

umbilical venous catheter is also affected by the degree and direction of liver displacement into the chest. Conversely, the location of umbilical artery catheters is rarely affected by CDH because of the retroperitoneal location of the aorta and its limited mobility (Figs. 5 and 6) [42].

Findings on initial chest radiograph, including the amount of aeration of the ipsilateral or contralateral lung, degree of mediastinal shift and hernia content, are not predictive of clinical outcome [43].

Other intrathoracic masses can mimic CDH (Fig. 7). When the diagnosis of CDH is in question, a small amount of contrast material or air can be injected via the nasogastric tube to outline the location of the bowel.

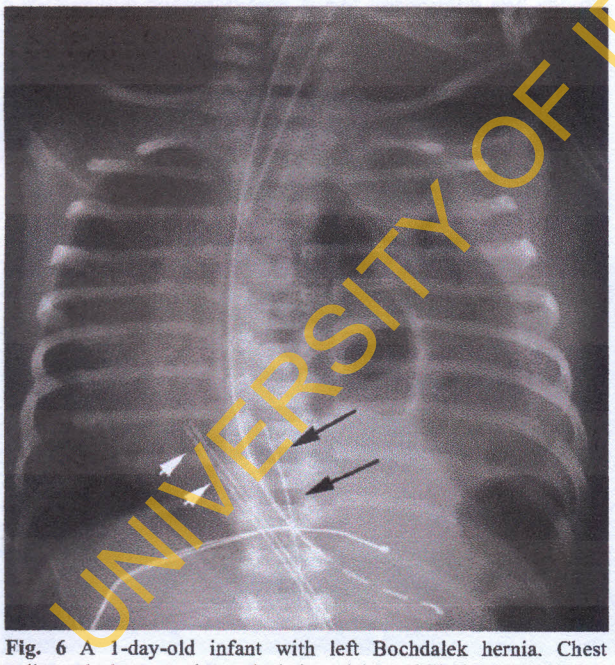

Fig. 6 A 1-day-old infant with left Bochdalek hernia. Chest radiograph shows moderate deviation of the umbilical venous catheter (*short arrows*) and minimal deviation of the umbilical artery catheter (*long arrows*) to the right

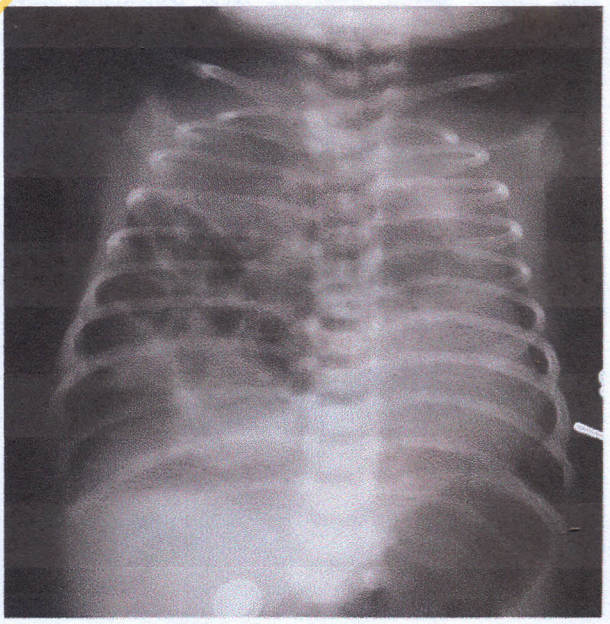

Fig. 7 A 3-day-old boy with congenital cystic adenomatoid malformation of right lung. Chest radiograph shows air-filled cysts that mimic intrathoracic bowel herniation

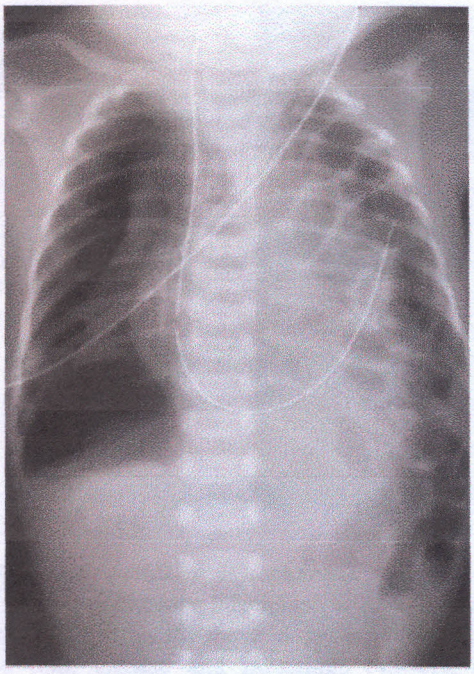

Fig. 8 A 1-hour-old infant with a large left Bochdalek hernia and right-side tension pneumothorax. Chest radiograph shows minimal mediastinal displacement by herniated bowel in the left chest

Lack of a mediastinal shift might be caused by a contralateral pneumothorax seen in infants with marked pulmonary hypoplasia and vigorous bag positive pressure ventilation (Fig. 8). However, after hernia repair, a large postoperative pneumothorax is not uncommon and should not be rapidly evacuated. Because of the increased mobility of the neonatal mediastinum, rapid evacuation of a pneumothorax may cause mediastinal rotation with torsion and obstruction of the venae cavae. Slow resorption of the pneumothorax allows a more gradual movement of mediastinal structures into a more normal position (Fig. 9). After the resorption of air surrounding the hypoplastic lung, fluid might accumulate in the pleural space.

Fluoroscopy can play an adjunctive role in selected patients in whom an eventration is suspected. Diminished respiratory excursion or paradoxical motion of the hemidiaphragm might be present in infants with thinning and poor muscularization of the diaphragm.

Cross-sectional imaging can be helpful in cases where the diagnosis is still not clear, and to fully elucidate the spectrum of associated anatomic defects. Sonography with color Doppler might be helpful in detecting an abnormal location or compromise of the superior mesenteric and portal vasculature, and in the identification of herniated solid viscera (Fig. 10). CT with multiplanar reconstruction is useful to elucidate associated lung masses and bronchopulmonary foregut malformations. The use of intravenous contrast agent and CT arteriography should be considered for depiction of the vascular supply of lung lesions. However, the administration of oral contrast material should be avoided because it can increase the degree of mediastinal shift and subsequent respiratory compromise. In stable patients, MRI can be used in the evaluation of complex lesions, as well.

Follow-up chest imaging after surgical repair might be useful to evaluate the functional consequences of the underlying pulmonary hypoplasia and its complications. Pulmonary hypoplasia will be manifest by the presence of a smaller lung with diminished pulmonary vascularity. Although pulmonary perfusion is often reduced on pulmonary scintigraphy, ventilation might remain relatively unaffected (Fig. 11) [44]. Several studies have looked at the long-term respiratory status of children after repair of CDH. Outcome appears to be related to the degree of pulmonary hypoplasia and need for extracorporeal membrane oxygenation (ECMO) in the neonatal period. Those children with milder forms of pulmonary

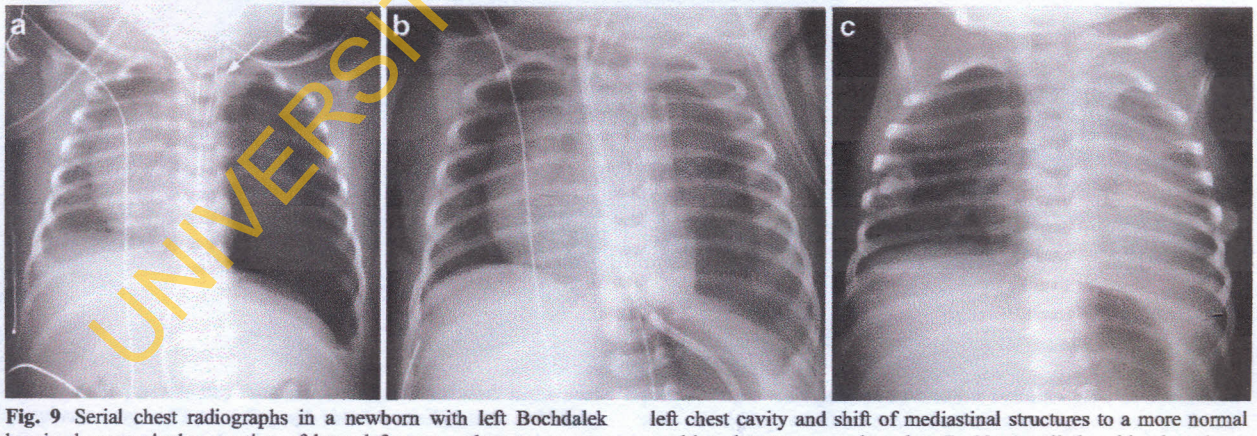

Fig. 9 Serial chest radiographs in a newborn with left Bochdalek hernia show gradual resorption of large left pneumothorax, progressive expansion of hypoplastic left lung, accumulation of fluid into the left chest cavity and shift of mediastinal structures to a more normal position by postoperative day 7. Note coiled epidural catheter (*arrows*). **a** Postrepair day 1. **b** Postrepair day 3. **c** Postrepair day 7

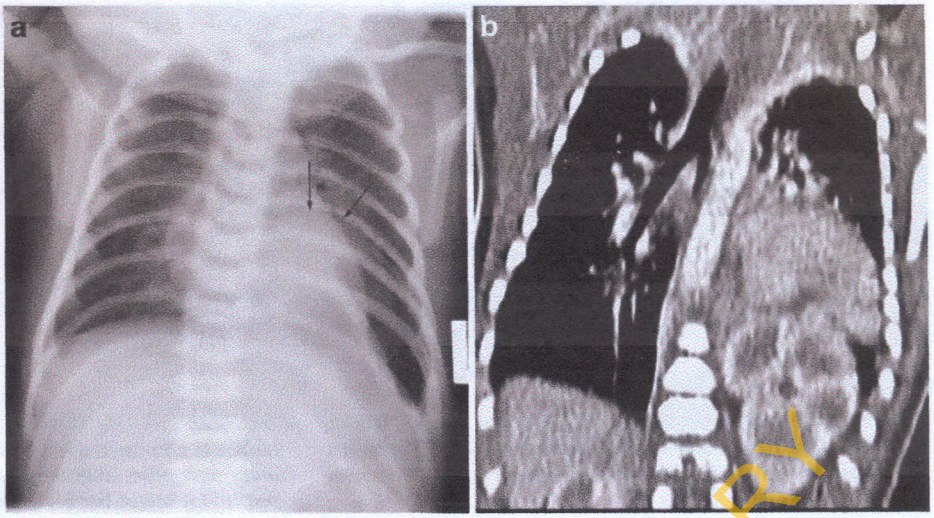

Fig. 10 A 4-day-old infant with a Bochdalek defect and herniation of solid viscera presenting with mild respiratory distress. **a** Chest radiograph shows bowel in the left hemithorax and a soft-tissue retrocardiac mass (*arrows*). **b** Coronal reconstructed, contrast-enhanced CT image shows intrathoracic herniation of the spleen and left kidney through a large Bochdalek hernia

hypoplasia are generally asymptomatic and are at no higher risk of pulmonary infections, while children who required ECMO therapy have a higher prevalence of chronic lung disease and infections [45–47]. Other complications include hernia recurrence (Fig. 12) and deformities of the spine (scoliosis) and chest wall (pectus excavatum or carinatum) [48, 49].

Treatment

The philosophy of initial management of CDH has changed during the last 20 years away from emergent to elective repair of the diaphragmatic defect. A number of studies have shown that medical management designed to address the major causes of neonatal mortality (pulmonary hypoplasia and pulmonary hypertension), followed by surgical repair, has led to improved outcomes [50–52]. Since 1995, a strategy of "gentle ventilation" consisting of permissive hypercapnia and spontaneous respiration has led to improved survival and less need for ECMO [53]. Additional ventilatory support strategies including high-frequency ventilation, nitric oxide inhalation, ECMO, and exogenous surfactant administration have been used with the goals of maintaining adequate oxygenation while minimizing lung damage [47, 50–52].

Surgical repair is accomplished via an abdominal approach with removal of abdominal viscera from the chest and primary repair of the defect (Fig. 13). Use of a fabric patch might be necessary in larger defects, and occasionally a split abdominal wall muscle flap is used when primary closure is not possible [54].

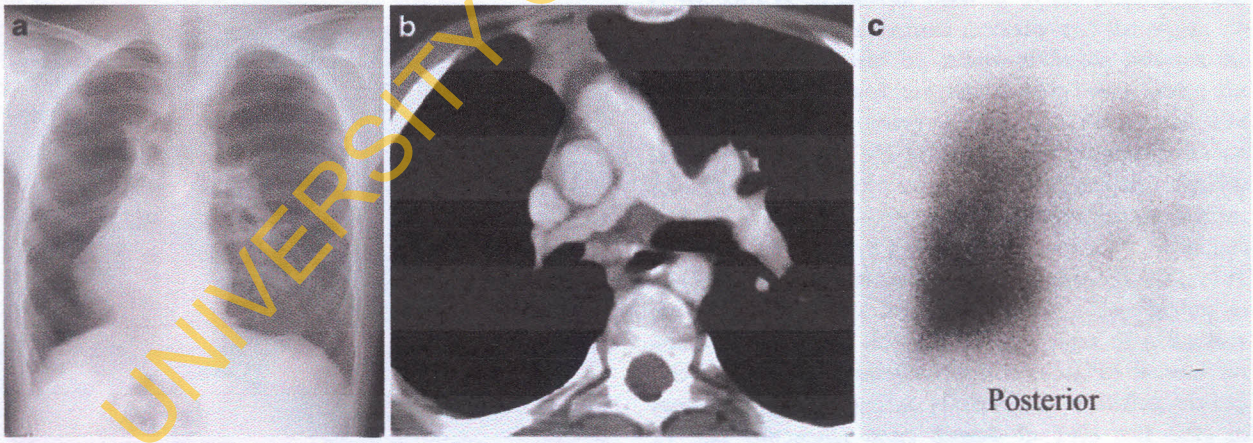

Fig. 11 A 12-year-old boy with repaired right Bochdalek hernia and hypoplastic lung. **a** Chest radiograph shows a small, lucent right lung and asymmetric increased pulmonary vascularity to the left lung. **b** Contrast-enhanced CT scan with mediastinal windows shows hypoplasia of right main pulmonary artery. **c** Posterior view of a perfusion scan of the lungs confirms marked asymmetry of pulmonary perfusion with 93% of total pulmonary flow to the left lung

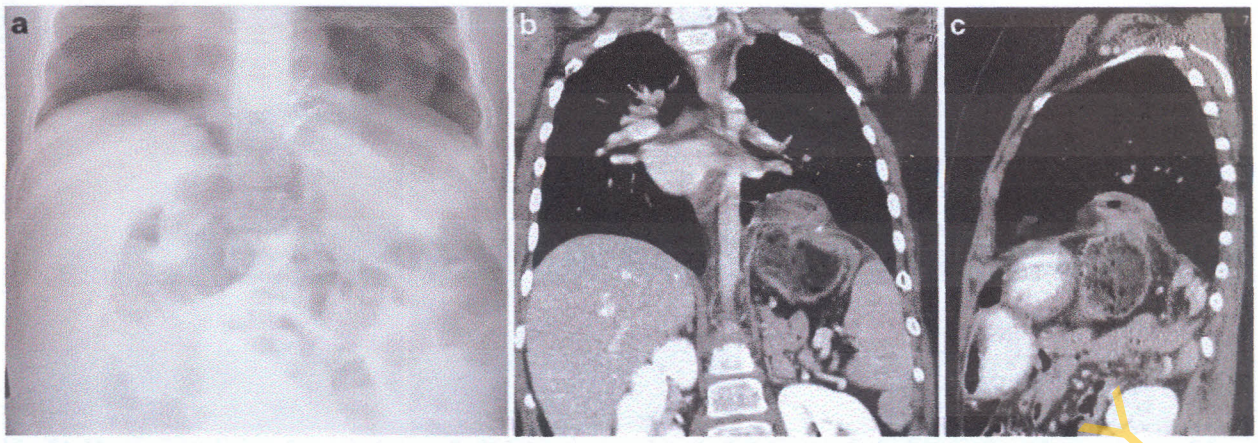

Fig. 12 A 7-year-old boy with neonatal patch repair of a Bochdalek hernia and recurrent defect. **a** Upper abdominal radiograph shows bowel loops in the left chest. **b**, **c** Coronal (**b**) and sagittal (**c**) contrast-enhanced CT reconstructions show a recurrent herniation of colon and mesentery through the medial and anterior lip of the patch repair

Outcomes

The prenatal diagnosis of CDH and the presence of associated malformations both contribute significantly to a very high "hidden mortality" rate in fetuses before they can reach an appropriate facility [55]. Thus, when the entire population of patients with CDH is evaluated, the overall mortality for CDH does not appear to have changed despite the advent of new therapies. However, once an infant with CDH is born and reaches a treatment facility, survival rates in selected, high-volume centers have steadily improved. Downard et al. [50] have reported a steady increase in survival rates for infants with CDH treated in Boston from 67% in 1998 to 93% in 2001. This has not been the experience in other countries. In a review of 185 cases of CDH in a regional case registry in the United Kingdom, Stege et al. [2] have reported survival rates ranging from 43% to 65% that were independent of the availability of ECMO, high-frequency ventilation, inhaled nitric oxide and delayed surgery. They conclude that reports of improved survival of CDH are likely to be explained by case selection and should be interpreted with caution [2].

After successful repair, patients with CDH continue to have a high prevalence of medical problems, including gastroesophageal reflux, developmental delay, poor growth, hearing loss, and musculoskeletal abnormalities (scoliosis and sternal deformities) [56].

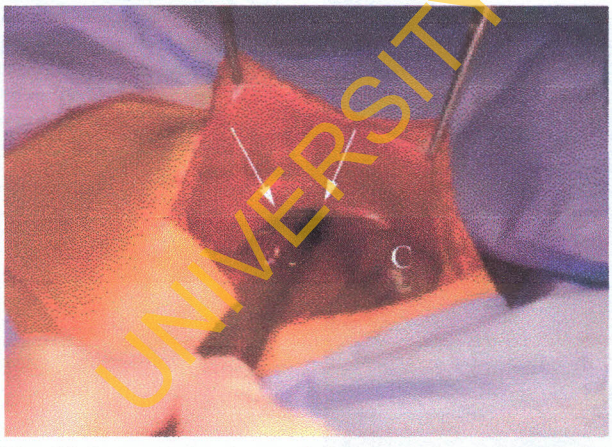

Fig. 13 Intraoperative image during surgical repair of a left Bochdalek hernia. View through a left transverse incision shows the colon (*C*) entering the chest though a large defect (*arrows*)

Retrosternal hernia

Anterior retrosternal hernias occur in two forms. The most common is a hernia through the foramen of Morgagni (FM). This is an anterior opening of the diaphragm that extends between the sternum medially and the eighth rib laterally and is caused by failure of fusion between the transverse septum and the lateral body wall where the internal mammary artery crosses the diaphragm. FM hernias account for 9% to 12% of diaphragmatic defects in infancy, are most commonly unilateral, and are right-side in 90% of cases [57–59]. Unlike Bochdalek-type hernias, most FM hernias have a well-defined hernia sac. Although FM hernias are occasionally diagnosed prenatally (Fig. 14), the majority of these hernias present in older children or adults as incidental findings, or with signs of pulmonary infection or gastrointestinal obstruction. FM hernias are associated with a number of anomalies including trisomy 21 and congenital heart disease in 14% and 58% of patients, respectively [60, 61]. Because of the risk of bowel incarceration and strangulation, these hernias should be repaired soon after diagnosis. Surgical repair consists of

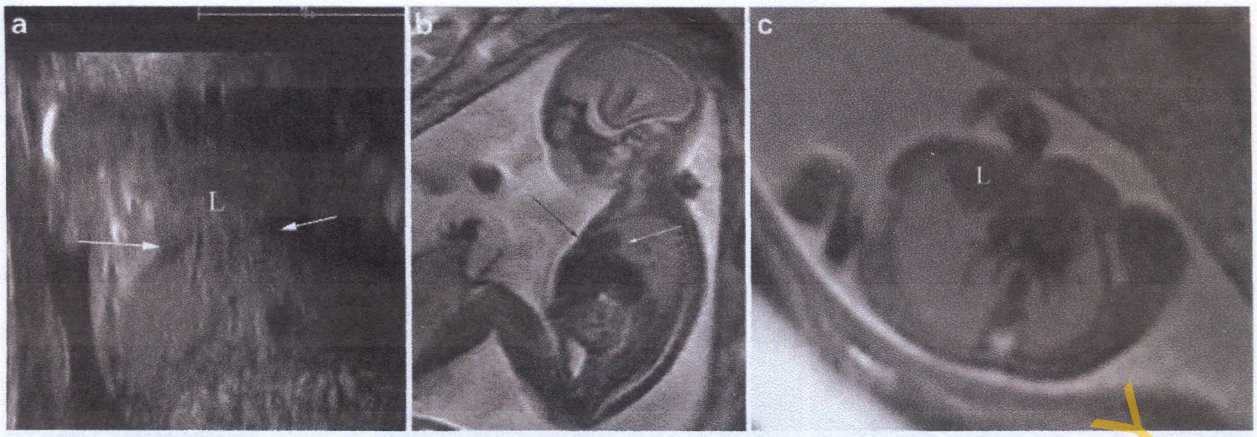

Fig. 14 Morgagni hernia in a 20-week fetus. **a** Sagittal sonogram through the right fetal chest shows herniation of the liver (*L*) into the chest; *arrows* depict the hernia. **b**, **c** Sagittal (**b**) and axial (**c**) T2-W images through the fetal chest confirm the herniation of liver (**b** *arrows*, **c** *L*) via an anterior foramen of Morgagni hernia

primary repair of the hernia by either an open transabdominal approach or by laparoscopic techniques.

The radiographic diagnosis is typically made when anterior herniation of bowel loops is identified on the lateral chest radiograph (Fig. 15). Other commonly herniated viscera include the liver, spleen and omentum, and might present as a medially located mass in the low anterior mediastinum. US or CT scan can be helpful when only solid abdominal viscera herniate (Fig. 16) [58]. The echotexture of herniated liver might be altered because of edema caused by vascular compression by a diaphragmatic defect (Fig. 17).

The second form of retrosternal hernia happens as a component of the pentalogy of Cantrell. This entity includes a number of congenital defects including omphalocele, inferior sternal cleft, complex cardiac defects, ectopia cordis, diaphragmatic hernia, and pericardial defects (Fig. 18). The deformity results from a failure of development of the septum transversum of the primitive diaphragm and is associated with poor outcomes caused by underlying complex heart disease. Repair of the defect involves correction of the cardiac lesion as well as abdominal wall and diaphragm closure. A prosthetic patch is often required [57, 62].

Hiatal hernia

A hiatal hernia is defined as the protrusion of a portion of the stomach into the mediastinum through the esophageal hiatus of the diaphragm [3]. Three types of hiatal hernia are

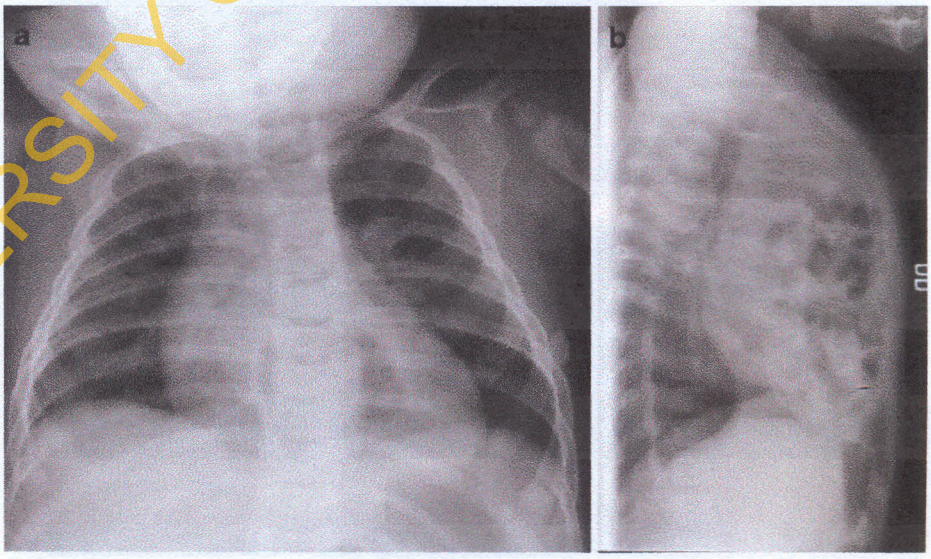

Fig. 15 A 2-week-old boy with Morgagni defect presenting with respiratory difficulty. Anteroposterior (**a**) and lateral (**b**) chest radiographs show intrathoracic bowel herniating through an anterior foramen of Morgagni defect

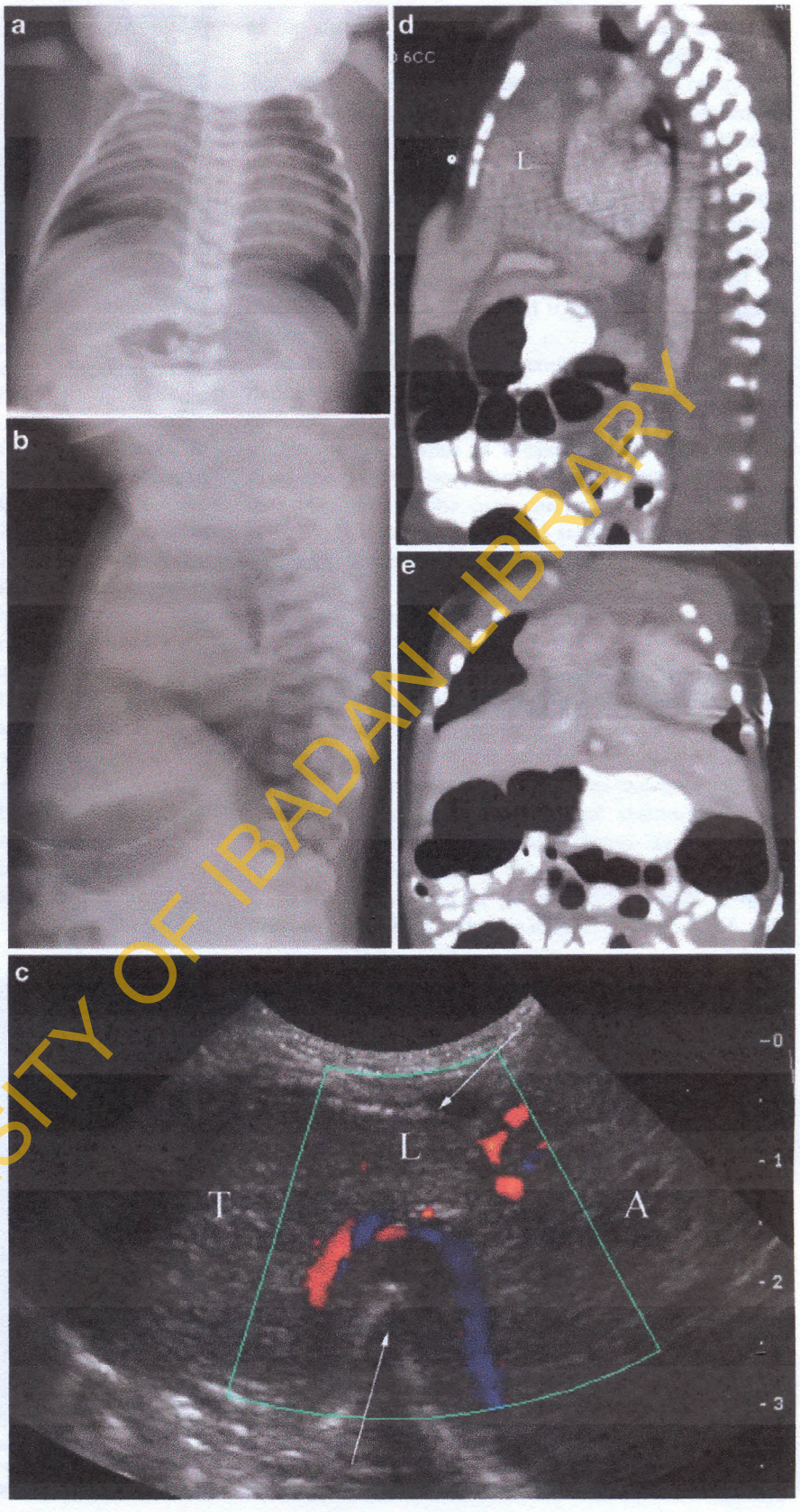

Fig. 16 A 7-day-old boy with a Morgagni hernia. **a**, **b** Antero-posterior (**a**) and lateral (**b**) chest radiographs show a poorly defined right chest mass and right upper lung atelectasis. **c** Sagittal color Doppler sonogram of the right chest obtained on the same day shows herniation of the liver (*L*) through an anterior foramen of Morgagni hernia (*arrows*). Note the abnormal course of the hepatic vein and the difference in echotexture of the intrathoracic (*T*) and intraabdominal (*A*) portions of the liver. **d**, **e** Sagittal (**d**) and coronal (**e**) contrast-enhanced CT reconstructions obtained the same day confirm anterior liver (*L*) herniation

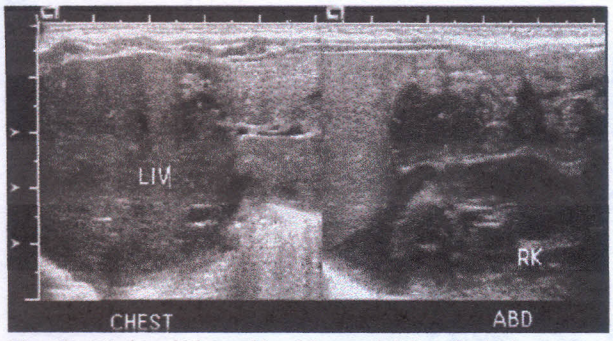

Fig. 17 A 1-day-old boy with a Morgagni defect. Sagittal sonogram of the right chest shows herniation of the liver through an anterior foramen of Morgagni defect. Note the lower echogenicity of the herniated portion of liver (*LIV*). *RK* right kidney

currently recognized (Fig. 19): sliding hiatus hernia, in which the esophagus moves freely through an enlarged hiatus into the chest; paraesophageal hernia, in which the gastroesophageal junction remains in its normal location and a portion of the stomach bulges through a hiatus anterior to the stomach; and congenital short esophagus, in which the stomach is irreducibly fixed in the chest. One potential explanation for the presence of congenital hiatal hernias relates to a delay in the descent of the stomach from the chest. The resulting esophageal hiatus is larger than normal, leaving a space between the esophagus and diaphragm [3]. Although hiatal hernias account for almost half of all hernias, the great majority of these are acquired lesions. Hiatal hernias account for only 9% of diaphragmatic hernias in infants younger than 1 year [59].

Prenatal diagnosis of a hiatal hernia might be possible by identification of a hypoechoic mass in the posterior mediastinum in continuity with the intraabdominal portion of the stomach [37]. Some of these cases are associated with a congenitally short esophagus that might cause a distended stomach to be located in the thoracic cavity.

Paraesophageal hernia is an uncommon but concerning entity in young children. These children are often missing the normal gastrosplenic and gastrocolic ligaments that anchor the stomach in the normal position. As a result, organoaxial volvulus of the stomach and colonic herniation can occur as serious complications [63]. Surgical repair involves reduction of herniated viscera followed by excision of the hernia sac, and tightening of the crura of the esophageal hiatus [64].

In infancy, larger hiatal hernias are visible on chest radiographs as a solid or air-filled retrocardiac mass (Fig. 20). A congenitally short esophagus might also be visible on radiographs as a cystic, space-occupying air-filled lesion in the chest. Identification of a nasogastric tube coursing through the cyst can suggest the diagnosis (Fig. 21). Upper gastrointestinal series with water-soluble contrast material will provide a definitive diagnosis.

Late-onset and acquired diaphragmatic hernia

Although the majority of children with CDH present during the first few days of life, late presentations have been reported as late as 12 years of age (Figs. 22 and 23). Older children with CDH often present with both acute and chronic gastrointestinal manifestations and less frequently respiratory symptoms [65]. Blunt abdominal trauma can also result in traumatic diaphragmatic hernia in older children. The diagnosis is missed on initial chest radiographs in up to 47% of patients. CT or MRI is often necessary to make a definitive diagnosis (Fig. 24) [66, 67].

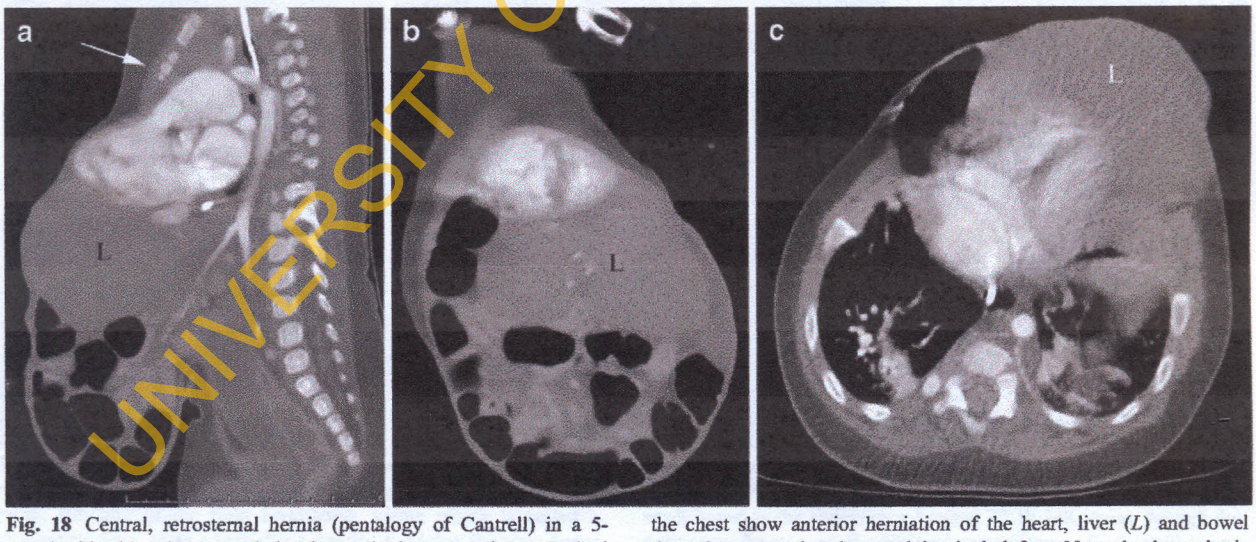

Fig. 18 Central, retrosternal hernia (pentalogy of Cantrell) in a 5-month-old with a large omphalocele repaired as a newborn. Sagittal (**a**), anterior coronal (**b**), and axial (**c**) contrast-enhanced CT images of the chest show anterior herniation of the heart, liver (*L*) and bowel through an anterior thoracoabdominal defect. Note the hypoplastic sternal ossification centers (**a** *arrow*)

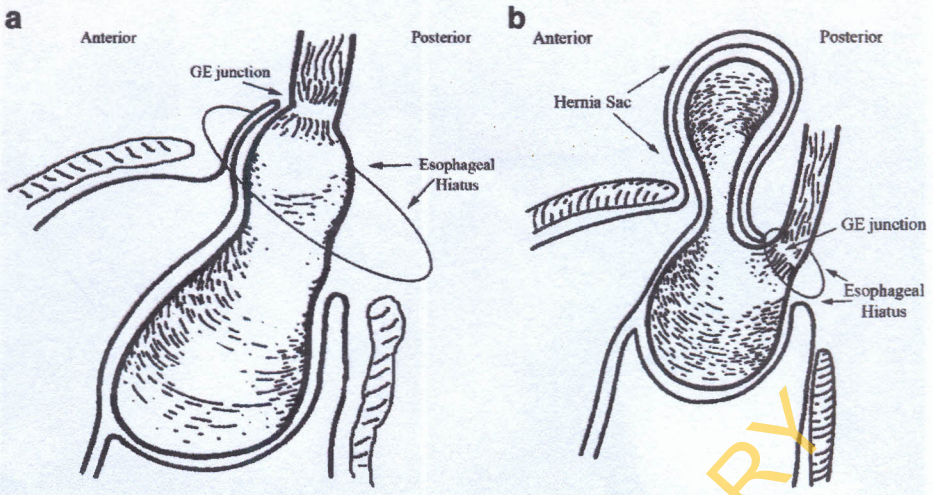

Fig. 19 Drawings of hiatal hernias. **a** Illustration of a sliding hiatal hernia shows an enlarged esophageal hiatus with elevation of the gastroesophageal junction and intrathoracic herniation of the stomach. **b** Illustration of a paraesophageal hernia shows a normal esophageal hiatus and gastroesophageal junction, and herniation of the stomach through an anterior hernia (diagrams modified from reference [4])

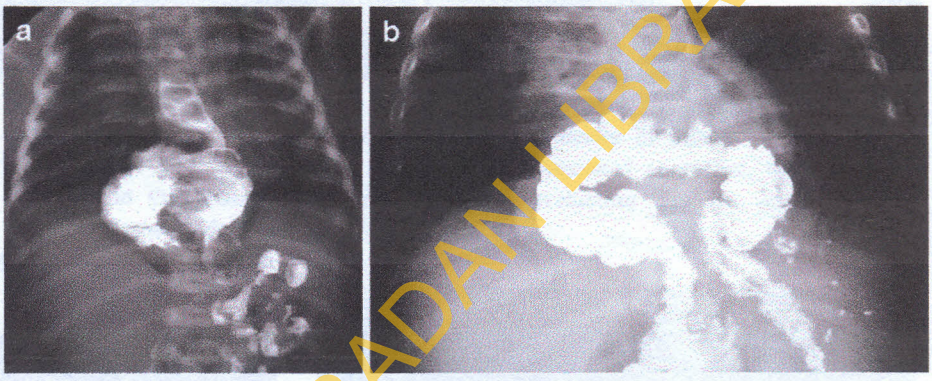

Fig. 20 A 4-month-old girl with a paraesophageal hernia who presented with vomiting. **a** Chest radiograph obtained during an upper gastrointestinal series shows intrathoracic herniation and organoaxial volvulus of the stomach into a paraesophageal hernia. **b** Delayed radiograph of the upper abdomen shows herniation of the transverse colon

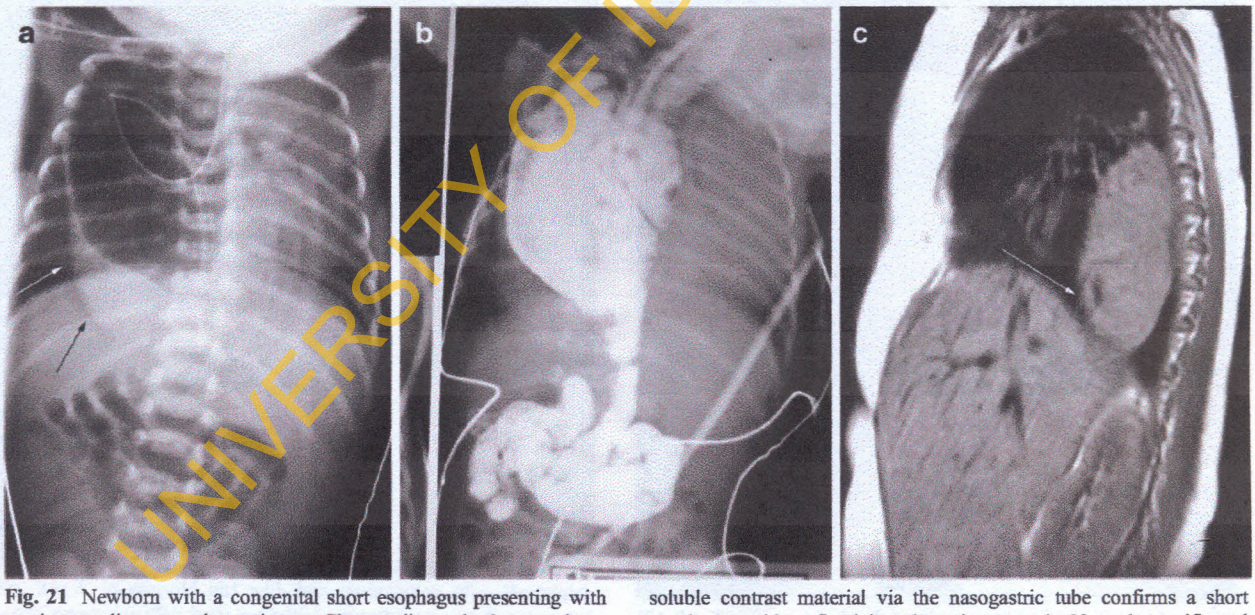

Fig. 21 Newborn with a congenital short esophagus presenting with respiratory distress and gagging. **a** Chest radiograph shows a large cystic structure in the right hemithorax within which is coiled a nasogastric tube. Note a lens-shape density overlying the right lower chest (*arrows*) **b** Radiograph obtained after administration of water-soluble contrast material via the nasogastric tube confirms a short esophagus with a fixed intrathoracic stomach. Note the malfixated small bowel in the abdomen. **c** Sagittal T2-W MR image through the right chest shows a small additional posterolateral (Bochdalek) hernia with liver herniation (*arrow*)

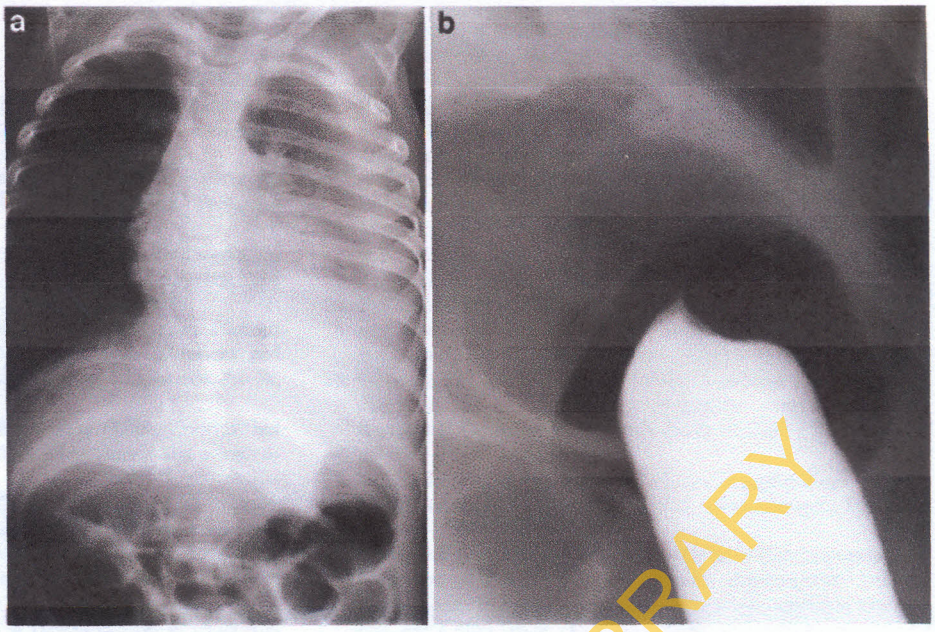

Fig. 22 A 2-year-old girl who presented with intermittent abdominal pain and mild shortness of breath caused by a small Bochdalek hernia. **a** Chest radiograph shows a moderate left plural effusion and mild small bowel dilatation. **b** Close-up image of the splenic flexure of the colon obtained during an enema using water-soluble contrast material shows a complete obstruction of the colon with a beak-like appearance. At surgery, ischemic colon was found in the left chest incarcerated by a 7-mm Bochdalek hernia

Conclusion

Imaging continues to play a key role in the prenatal detection and characterization of diaphragmatic defects and in the postnatal monitoring of ventilatory therapy in these complex and critically ill infants. Because of the high prevalence of associated anomalies, detailed multimodality imaging evaluation can be very useful in selected infants.

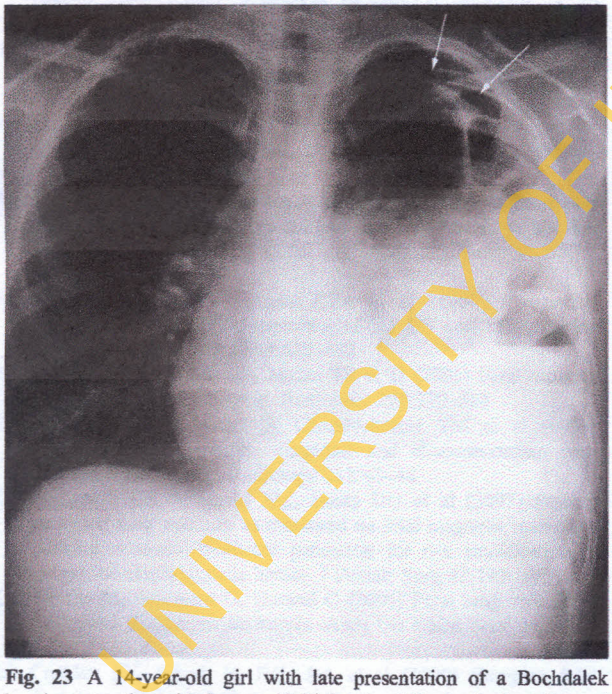

Fig. 23 A 14-year-old girl with late presentation of a Bochdalek hernia, presenting with fever and initial periumbilical pain that migrated to the left shoulder. Chest radiograph shows bowel in the left hemithorax and a pneumothorax (*arrows*). At surgery, a Bochdalek hernia and perforated appendix were identified in the left hemithorax

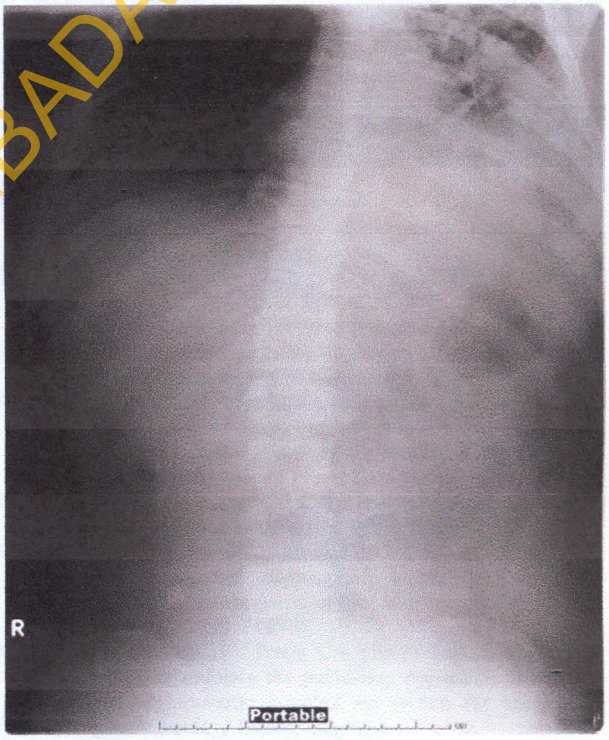

Fig. 24 Traumatic hernia of the diaphragm in a 15-year-old boy with acute chest pain and vomiting after competing in a cross-country race. Radiograph of the upper abdomen shows herniation of the bowel and malpositioned nasogastric tube in the left hemidiaphragm

References

1. Cohen MS, Rychik J, Bush DM et al (2002) Influence of congenital heart disease on survival in children with congenital diaphragmatic hernia. J Pediatr 141:25–30
2. Stege G, Fenton A, Jaffray B (2003) Nihilism in the 1990s: the true mortality of congenital diaphragmatic hernia. Pediatrics 112:532–535
3. Skandalakis JE, Gray SW, Ricketts RR (1994) The diaphragm. In: Skandalakis JE, Gray SW (eds) Embryology for surgeons, 2nd edn. Williams & Wilkins, Baltimore, pp 491–539
4. Stolar CJH (1997) Congenital diaphragmatic hernia. In: Oldham KT, Colombani PM, Foglia RP (eds) Surgery of infants and children: scientific principles and practice. Lippincott-Raven, Philadelphia, pp 883–895
5. Pringle KC, Turner JW, Schofield JC et al (1984) Creation and repair of diaphragmatic hernia: lung development and morphology. J Pediatr Surg 19:131–140
6. Clugston RD, Klattig J, Englert C et al (2006) Teratogen-induced, dietary and genetic models of congenital diaphragmatic hernia share a common mechanism of pathogenesis. Am J Pathol 169:1541–1549
7. Bielinska M, Jay PY, Erlich JM et al (2007) Molecular genetics of congenital diaphragmatic defects. Ann Med 39:261–274
8. Sharma S, Jain R, Singh MK et al (2007) A case of congenital diaphragmatic hernia with a hernia sac attached to the liver: hints for an early embryological insult. J Pediatr Surg 42:1761–1763
9. Greer JJ, Cote D, Allan DW et al (2000) Structure of the primordial diaphragm and defects associated with nitrofen-induced CDH. J Appl Physiol 89:2123–2129
10. Babiuk RP, Greer JJ (2002) Diaphragm defects occur in a CDH hernia model independently of myogenesis and lung formation. Am J Physiol Lung Cell Mol Physiol 283:L1310–L1314
11. Garne E, Haeusler M, Barisic I et al (2002) Congenital diaphragmatic hernia: evaluation of prenatal diagnosis in 20 European regions. Ultrasound Obstet Gynecol 19:329–333
12. Seaward GR (2005) The fetal chest. In: Rumack CM, Wilson SR, Charboneau JW (eds) Diagnostic ultrasound, 3rd edn. Elsevier Mosby, St. Louis, pp 1303–1321
13. Bootstaylor BS, Filly RA, Harrison MR et al (1995) Prenatal sonographic predictors of liver herniation in congenital diaphragmatic hernia. J Ultrasound Med 14:515–520
14. Ruano R, Benachi A, Joubin L et al (2004) Three-dimensional ultrasonographic assessment of fetal lung volume as prognostic factor in isolated congenital diaphragmatic hernia. BJOG 111:423–429
15. Jani JC, Cannie M, Peralta CFA et al (2007) Congenital diaphragmatic hernia: comparison of 3D US and MR imaging assessments. Radiology 244:575–582
16. Levine D, Barnewolt CE, Mehta TS et al (2003) Fetal thoracic abnormalities: MR imaging. Radiology 228:379–388
17. Hubbard AM, Adzick NS, Crombleholme TM et al (1999) Congenital chest lesions: diagnosis and characterization with prenatal MR imaging. Radiology 212:43–48
18. Barnewolt CE, Kunisaki SM, Fauza DO et al (2007) Percent predicted lung volumes as measured on fetal magnetic resonance imaging: a useful biometric parameter for risk stratification in congenital diaphragmatic hernia. J Pediatr Surg 42:193–197
19. Bonfils M, Emeriaud G, Durand C (2006) Fetal lung volume in congenital diaphragmatic hernia. Arch Dis Child Fetal Neonatal Ed 91:F363–F364
20. Coakley FV, Hricak H, Filly RA et al (1999) Complex fetal disorders: effect of MR imaging on management – preliminary clinical experience. Radiology 213:691–696
21. Rypens F, Metens T, Rocourt N et al (2001) Fetal lung volume: estimation at MR imaging – initial results. Radiology 219:236–241
22. Büsing KA, Kilian K, Schaible T et al (2007) Reliability and validity of MR image lung volume measurement in fetuses with congenital diaphragmatic hernia and in vitro lung models. Radiology 246:553–561
23. Enns GM, Cox VA, Goldstein RB et al (1998) Congenital diaphragmatic defects and associated syndromes, malformations, and chromosome anomalies: a retrospective study of 60 patients and literature review. Am J Med Genet 79:215–225
24. Migliazza L, Otten C, Xia H et al (1999) Cardiovascular malformations in congenital diaphragmatic hernia: human and experimental studies. J Pediatr Surg 34:1352–1358
25. Fauza DO, Wilson JM (1994) Congenital diaphragmatic hernia and associated anomalies: their incidence, identification, and impact on prognosis. J Pediatr Surg 29:1113–1117
26. Graziano JN (2005) Cardiac anomalies in patients with congenital diaphragmatic hernia and their prognosis: a report from the Congenital Diaphragmatic Hernia Study Group. J Pediatr Surg 40:1045–1049
27. Grethel EJ, Farrell J, Ball R et al (2007) Congenital diaphragmatic hernia associated with spinal anomalies. Obstet Gynecol 209:485–488
28. Slavotinek AM, Warmerdam B, Lin AE et al (2007) Population-based analysis of left- and right-sided diaphragmatic hernias demonstrates different frequencies of selected additional anomalies. Am J Med Genet 143A:3127–3136
29. Witters I, Legius E, Moerman P et al (2001) Associated malformations and chromosomal anomalies in 42 cases of prenatally diagnosed diaphragmatic hernia. Am J Med Genet 103:278–282
30. Metkus AP, Filly RA, Stringer MD et al (1996) Sonographic predictors of survival in fetal diaphragmatic hernia. J Pediatr Surg 31:148–151
31. Walsh DS, Hubbard AM, Olutoye OO et al (2000) Assessment of fetal lung volumes and liver herniation with magnetic resonance imaging in congenital diaphragmatic hernia. Am J Obstet Gynecol 183:1067–1069
32. Laudy JAM, Van Gucht M, van Dooren MF et al (2003) Congenital diaphragmatic hernia: an evaluation of the prognostic value of the lung-to-head ratio and other prenatal parameters. Prenat Diagn 23:634–639
33. Datin-Dorriere V, Rouzies S, Taupin P et al (2008) Prenatal prognosis in isolated congenital diaphragmatic hernia. Am J Obstet Gynecol 198:80.e1–80.e5
34. Sbragia L, Paek BW, Filly RA et al (2000) Congenital diaphragmatic hernia without herniation of the liver: does the lung-to-head ratio predict survival? J Ultrasound Med 19:845–848
35. O'Rourke PP (1993) Congenital diaphragmatic hernia: are there reliable clinical predictors? Crit Care Med 21:S380–S381
36. Hedrick H, Danzer E, Merchant A et al (2007) Liver position and lung-to-head ratio for prediction of extracorporeal membrane oxygenation and survival in isolated left congenital diaphragmatic hernia. Am J Obstet Gynecol 197:422.e1–422.e4
37. Ruano R, Benachi A, Aubry M-C et al (2003) Prenatal sonographic diagnosis of congenital hiatal hernia. Prenat Diagn 24:26–30
38. Gorincour G, Bouvenot J, Mourot MG et al (2005) Prenatal prognosis of congenital diaphragmatic hernia using magnetic resonance imaging measurement of fetal lung volume. Ultrasound Obstet Gynecol 26:738–744
39. Wilson J, DiFiore JW, Peters CA (1993) Experimental fetal tracheal ligation prevents the pulmonary hypoplasia associated with fetal nephrectomy: possible application for congenital diaphragmatic hernia. J Pediatr Surg 28:1433–1439
40. DiFiore JW, Fauza DO, Slavin R et al (1994) Experimental fetal tracheal ligation reverses the structural and physiological effects of pulmonary hypoplasia in congenital diaphragmatic hernia. J Pediatr Surg 29:248–256

41. Bohn D (2006) Diaphragmatic hernia – pre and postnatal. Paediatr Respir Rev 7 [Suppl 1]:S249–S250
42. Sakurai M, Donnelly LF, Klosterman LA et al (2000) Congenital diaphragmatic hernia in neonates: variations in umbilical catheter and enteric tube position. Radiology 216:112–116
43. Holt PD, Arkovitz MS, Berdon WE et al (2004) Newborns with diaphragmatic hernia: initial chest radiography does not have a role in predicting clinical outcome. Pediatr Radiol 34:462–464
44. Treves ST, Packard AB (2007) Lungs. In: Treves ST (ed) Pediatric nuclear medicine, 3rd edn. Springer, New York, pp 87–127
45. Wohl ME, Griscom NT, Strieder DJ et al (1977) The lung following repair of congenital diaphragmatic hernia. J Pediatr 90:405–414
46. Falconer AR, Brown RA, Helms P et al (1990) Pulmonary sequelae in survivors of congenital diaphragmatic hernia. Thorax 45:126–129
47. Van Meurs KP, Newman KD, Anderson KD et al (1990) Effect of extracorporeal membrane oxygenation on survival of infants with congenital diaphragmatic hernia. J Pediatr 117:954–960
48. Trachsel D, Selvadurai H, Bohn D et al (2005) Long-term pulmonary morbidity in survivors of congenital diaphragmatic hernia. Pediatr Pulmonol 39:433–439
49. Rais-Bahrami K, Robbins ST, Reed VL et al (1995) Congenital diaphragmatic hernia. Outcome of preoperative extracorporeal membrane oxygenation. Clin Pediatr (Phila) 34:471–474
50. Downard CD, Jaksic T, Garza JJ et al (2003) Analysis of an improved survival rate for congenital diaphragmatic hernia. J Pediatr Surg 38:729–732
51. Frenckner B, Ehren H, Granholm T et al (1997) Improved results in patients who have congenital diaphragmatic hernia using preoperative stabilization, extracorporeal membrane oxygenation, and delayed surgery. J Pediatr Surg 32:1185–1189
52. Boloker J, Bateman DA, Wung JT et al (2002) Congenital diaphragmatic hernia in 120 infants treated consecutively with permissive hypercapnea/spontaneous respiration/elective repair. J Pediatr Surg 37:357–366
53. Brown RA, Bösenberg AT (2007) Evolving management of congenital diaphragmatic hernia. Paediatr Anaesth 17:713–719
54. Brant-Zawadzki PB, Fenton SJ, Nichol PF et al (2007) The split abdominal wall muscle flap repair for large congenital diaphragmatic hernias on extracorporeal membrane oxygenation. J Pediatr Surg 42:1047–1050
55. Skari H, Bjornland K, Egeland T et al (2000) Congenital diaphragmatic hernia: a meta-analysis of mortality factors. J Pediatr Surg 35:1187–1197
56. Lund DP, Mitchell J, Kharasch V et al (1994) Congenital diaphragmatic hernia: the hidden morbidity. J Pediatr Surg 29:258–262
57. Arensman RM, Bambini DA (2000) Congenital diaphragmatic hernia and eventration. In: Ashcraft KW (ed) Pediatric surgery, 3rd edn. Saunders, Philadelphia, pp 300–317
58. Robnett-Filly B, Goldstein RB, Sampior D et al (2003) Morgagni hernia. A rare form of congenital diaphragmatic hernia. J Ultrasound Med 22:537–539
59. Karpelowsky JS, Wieselthaler N, Rode H (2006) Primary paraesophageal hernia. J Pediatr Surg 41:1588–1593
60. Pokorny W, McGill C, Halberg F (1984) Morgagni hernia during infancy: presentation and associated anomalies. J Pediatr Surg 19:394–397
61. de Fonseca J, Davies M, Bolton K (1987) Congenital hydropericardium associated with the herniation of part of the liver into the pericardial sac. J Pediatr Surg 22:851–853
62. Cantrell J, Haller J, Ravitch M (1958) A syndrome of congenital defects involving the abdominal wall, sternum, diaphragm, pericardium and heart. Surg Gynecol Obstet 107:602–614
63. Imamoglu M, Çay A, Kosucu P et al (2005) Congenital paraesophageal hiatal hernia: pitfalls in the diagnosis and treatment. J Pediatr Surg 40:112–113
64. Al-Salem AH (2000) Congenital paraesophageal hernia in infancy and childhood. Saudi Med J 21:164–167
65. Mei-Zahav M, Solomon M, Trachsel D et al (2003) Bochdalek diaphragmatic hernia: not only a neonatal disease. Arch Dis Child 88:532–535
66. Ramos CT, Koplewits BZ, Babyn PS et al (2000) What have we learned about traumatic diaphragmatic hernias in children? J Pediatr Surg 35:601–604
67. Cigdem MK, Onen A, Otcu S et al (2007) Late presentation of Bochdalek-type congenital diaphragmatic hernia in children: a 23-year experience at a single center. Surg Today 37:642–645